



PAPER • OPEN ACCESS

Ultracold neutron storage simulation using the Kassiopeia software package

To cite this article: Z Bogorad *et al* 2022 *New J. Phys.* **24** 023007

View the [article online](#) for updates and enhancements.

You may also like

- [Fundamental interactions involving neutrons and neutrinos: reactor-based studies led by Petersburg Nuclear Physics Institute \(National Research Centre 'Kurchatov Institute'\) \[PNPI \(NRC KI\)\]](#)
A P Serebrov
- [Study of levitating nanoparticles using ultracold neutrons](#)
V V Nesvizhevsky, A Yu Voronin, A Lambrecht *et al.*
- [Disagreement between measurements of the neutron lifetime by the ultracold neutron storage method and the beam technique](#)
A P Serebrov



PAPER

Ultracold neutron storage simulation using the Kassiopeia software package

OPEN ACCESS

RECEIVED
29 June 2021REVISED
31 December 2021ACCEPTED FOR PUBLICATION
12 January 2022PUBLISHED
9 February 2022Z Bogorad^{1,2}, P Mohanmurthy^{1,3,*}  and J A Formaggio¹ ¹ Laboratory for Nuclear Science, Massachusetts Institute of Technology, Cambridge, MA 02139, United States of America² Stanford Institute for Theoretical Physics, Stanford University, Stanford, CA 94305, United States of America³ University of Chicago, Chicago, IL 60637, United States of America

* Author to whom any correspondence should be addressed.

E-mail: prajwal@mohanmurthy.com**Keywords:** simulations, ultracold neutrons, particle tracking, spin tracking, software

Original content from
this work may be used
under the terms of the
[Creative Commons
Attribution 4.0 licence](https://creativecommons.org/licenses/by/4.0/).

Any further distribution
of this work must
maintain attribution to
the author(s) and the
title of the work, journal
citation and DOI.



Abstract

The Kassiopeia software package was originally developed to simulate electromagnetic fields and charged particle trajectories for neutrino mass measurement experiments. Recent additions to Kassiopeia also allow it to simulate neutral particle trajectories in magnetic fields based on their magnetic moments. Two different methods were implemented: an exact method that can work for arbitrary fields and an adiabatic method that is limited to slowly-varying fields but is much faster for large precession frequencies. Additional interactions to simulate reflection of ultracold neutrons (UCNs) from material walls and to allow spin–flip pulses were also added. These tools were used to simulate neutron precession in a room temperature neutron electric dipole moment experiment and predict the values of the longitudinal and transverse relaxation times as well as the trapping lifetime. All three parameters are found to closely match the experimentally determined values when simulated with both the exact and adiabatic methods, confirming that Kassiopeia is able to accurately simulate neutral particles. This opens the door for future uses of Kassiopeia to prototype the next generation of atomic traps and UCN experiments.

1. Introduction

At sufficiently low energies, neutrons can be reflected from material walls by the coherent strong interaction [1–3]. Such neutrons can be stored in material traps, and are termed ultracold neutrons (UCNs).

The ability of UCNs to be stored for prolonged periods makes them of interest in several experimental areas. They can be used to measure the neutron lifetime [4, 5], which continues to be of interest due to the remaining discrepancy between different experimental measurements [6]. UCNs can also be used to constrain the neutron electric dipole moment, which is related to the strong CP problem and can constrain beyond the standard model physics [7–9]. Currently, the best upper bound on the neutron electric dipole moment comes from measurements on UCNs, described in [10].

Several software packages have previously been used to simulate UCNs, including Geant4 [11, 12], PENTrack [13], STARucn [14, 15] and MCUCN [16]. The topic of this paper, the Kassiopeia toolkit [17], provides particular set of advantages and additional options for the users. In this paper, we demonstrate the ability of Kassiopeia, a software package originally developed for neutrino experiments, to accurately simulate UCN storage. In section 2, we describe some general features of Kassiopeia, not specific to UCNs. We then describe neutral particle tracking features that have been added to Kassiopeia in order to simulate UCNs in section 3. Next, we describe a specific experiment that we simulated and the parameters of our simulation in section 4, and describe our results in section 5. In section 5, we have also highlighted the advantages of our toolkit and compared the processes used in vetting various other toolkits. Finally, in section 6 we consider possible future applications of Kassiopeia's neutral particle tracking capabilities.

2. Simulation in Kassiopeia

Kassiopeia was created as a combined field solver and particle tracker for the KATRIN collaboration [17]. It is developed in C++ using a modular design that allows it to be adapted to various applications using different field solvers, equations of motion and interactions. The standard distribution, available at <https://github.com/KATRIN-Experiment/Kassiopeia>, implements a variety of these features already, and Kassiopeia is designed for easy development of additional modules for future applications. Individual simulations can then be configured using an extensible markup language file.

Kassiopeia has several implemented methods to calculate the electromagnetic fields associated with a particular geometry. Magnetic fields can be calculated using zonal harmonic expansions [18], or the fast multipole method [19], while electric fields can be computed using the boundary element method [18]. Both types of fields can also be measured and imported, as is done in this work.

Kassiopeia also has several modules, called ‘trajectories’, for solving particles’ equations of motion. Different trajectories include different terms in the equations of motion and use different representations of particle states. Early versions of Kassiopeia included two main trajectory modules: an exact trajectory module, which describes particles via their position and momentum in laboratory coordinates and is limited only by the integration step size, and an adiabatic trajectory module, which calculates and records particles’ position and motion around the magnetic field lines that they adiabatically follow at sufficiently low energies.

Both of these modules implemented equations of motion that assumed a non-zero particle charge, which prevented Kassiopeia from simulating other particles of interest, such as neutrons or neutral atoms. To remedy this, two new trajectory modules were added to Kassiopeia: an exact spin trajectory and an adiabatic spin trajectory, described below. Both modules describe particles’ position and momentum in laboratory coordinates, as in the original exact trajectory, but then add additional terms based on particles’ magnetic moments, determined by their spins. These additional terms are potentially the only non-zero terms in the equations of motion for neutral particles.

3. Spin features in Kassiopeia

At each integration step of a trajectory calculation, two parameters of the particle’s evolution must be calculated: the time derivative of the spin, and the force on the particle as a function of the spin and surrounding fields. We therefore next describe how these are calculated for the exact spin trajectory.

The relativistic generalization of a classical spin is the four-vector $S = (S_0, \mathbf{S})$ given by, for a particle with classical spin \mathbf{s} and velocity $\mathbf{v} = \beta c$ and Lorentz factor Γ (to avoid confusion with the gyromagnetic ratio γ) [25],

$$S_0 = \Gamma \boldsymbol{\beta} \cdot \mathbf{s}, \quad (1a)$$

$$\mathbf{S} = \mathbf{s} + \frac{\Gamma^2}{\Gamma + 1} (\boldsymbol{\beta} \cdot \mathbf{s}) \boldsymbol{\beta}. \quad (1b)$$

The equations of motion for a relativistic spin with four-velocity U^α in fields $F^{\mu\nu}$, using the particle’s proper time τ , are given by the BMT equation:

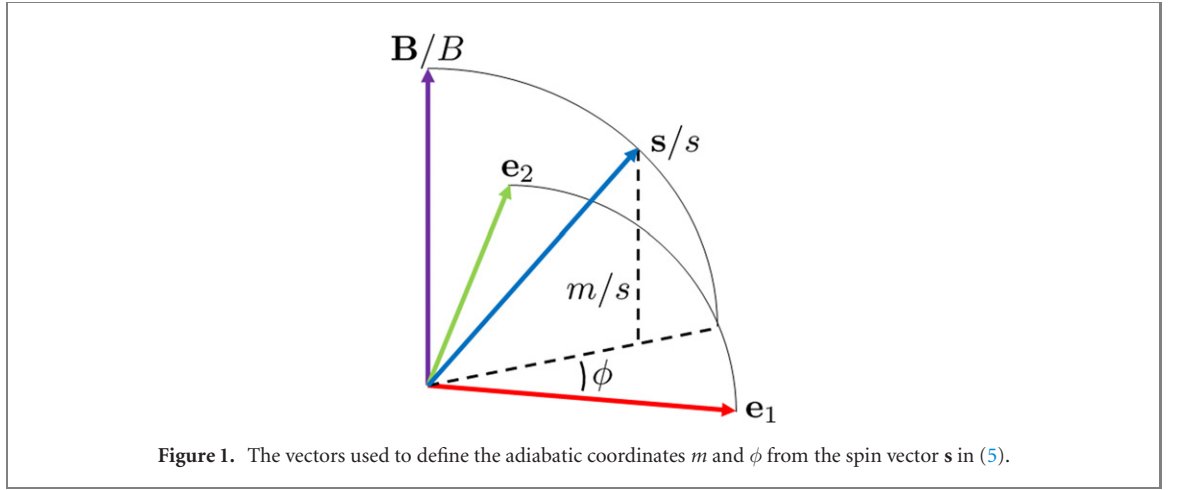
$$\frac{dS^\alpha}{d\tau} = \frac{\gamma}{c} \left[F^{\alpha\beta} S_\beta + \frac{1}{c^2} U^\alpha (S_\lambda F^{\lambda\mu} U_\mu) \right] - \frac{1}{c^2} U^\alpha \left(S_\lambda \frac{dU^\lambda}{d\tau} \right). \quad (2)$$

The spin-dependent contribution to the particle’s motion is given by the magnetic dipole force term, which is implemented nonrelativistically:

$$\mathbf{F} = \nabla(\gamma \mathbf{s} \cdot \mathbf{B}). \quad (3)$$

This exact spin tracking method is completely general, except for the assumption that relativistic corrections to the magnetic dipole force term are negligible. However, the step size for numerically integrating these equations of motion is limited by the precession rate of the spins, $\gamma |\mathbf{B}|$. This is typically fast relative to other timescales of a particle’s motion, which can make the exact spin tracking method impractically slow for experiments with long timescales.

Given the high computational cost of simulating tracks with the exact spin trajectory, an adiabatic spin trajectory was also implemented. The adiabatic spin trajectory records particle spins using two variables instead of four: an aligned spin m that gives the component of the spin along the magnetic field at the particle’s position, and a spin angle ϕ that gives the orientation of the spin around that field. This spin angle is defined with respect to two unit vectors orthogonal to the local magnetic field, \mathbf{e}_1 and \mathbf{e}_2 , defined, for a



magnetic field $\mathbf{B} = (B_x, B_y, B_z)$ in laboratory coordinates, as:

$$\mathbf{e}_1 := (B_z, 0, -B_x) / \sqrt{B_x^2 + B_z^2}, \quad (4a)$$

$$\mathbf{e}_2 := \mathbf{B} \times \mathbf{e}_1 / |\mathbf{B}|. \quad (4b)$$

Given these axes, ϕ gives the angle of the projection of the spin into the plane perpendicular to \mathbf{B} away from \mathbf{e}_1 , in the direction of \mathbf{e}_2 :

$$\mathbf{s} = (s^2 - m^2)^{1/2} (\mathbf{e}_1 \cos \phi + \mathbf{e}_2 \sin \phi) + m\mathbf{B}/|\mathbf{B}|. \quad (5)$$

The relationship between these vectors is illustrated in figure 1.

These two parameters, m and ϕ , along with the position \mathbf{x} , then give the adiabatic spin equations of motion (excluding contributions independent of spin) [26]:

$$\frac{M}{\hbar} \ddot{\mathbf{x}} = \gamma m \nabla |\mathbf{B}| + \gamma |\mathbf{B}| (s^2 - m^2)^{1/2} \nabla \mathbf{b} \cdot \mathbf{c}, \quad (6a)$$

$$\frac{\dot{m}}{s} = (s^2 - m^2)^{1/2} (\dot{\mathbf{x}} \cdot \nabla \mathbf{b} \cdot \mathbf{c}), \quad (6b)$$

$$\dot{\phi} = -\gamma |\mathbf{B}| - \dot{\mathbf{x}} \cdot \mathbf{A} - \frac{sm}{(s^2 - m^2)^{1/2}} (\dot{\mathbf{x}} \cdot \nabla \mathbf{b} \cdot \mathbf{a}), \quad (6c)$$

where \mathbf{x} is position, γ is the particle's gyromagnetic ratio, M is its mass, s is the magnitude of its total spin, and we have defined:

$$\mathbf{a} = -\mathbf{e}_1 \cos \phi + \mathbf{e}_2 \sin \phi, \quad (7a)$$

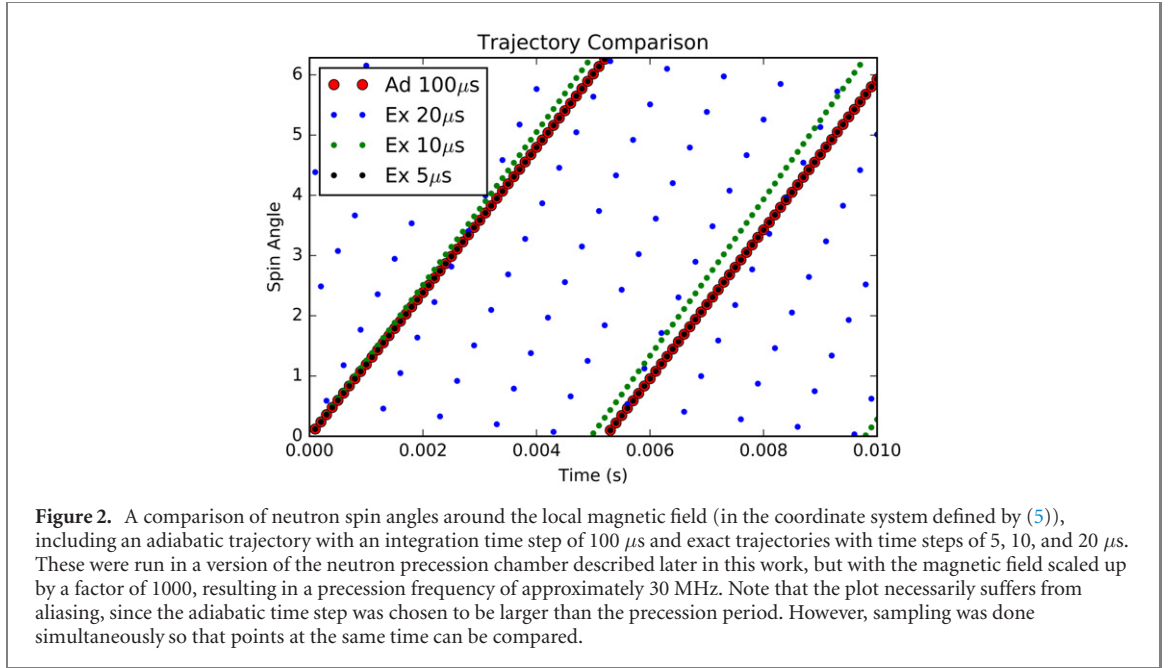
$$\mathbf{b} = \mathbf{B}/|\mathbf{B}|, \quad (7b)$$

$$\mathbf{c} = \mathbf{e}_1 \cos \phi + \mathbf{e}_2 \sin \phi, \quad (7c)$$

$$\mathbf{A} = \nabla \mathbf{e}_1 \cdot \mathbf{e}_2. \quad (7d)$$

for convenience.

This adiabatic spin trajectory is accurate when particles are non-relativistic and spin precession is fast compared to the rate at which the field at the particle's location changes. Assuming the spin precession rate is dominated by the first term $\gamma |\mathbf{B}|$, this requires $\gamma |\mathbf{B}| \gg |\dot{\mathbf{x}} \cdot \nabla \mathbf{B}|/|\mathbf{B}|$, which should hold for all applications discussed in this work. During a single integration time step, the exact trajectory requires the spin to rotate by much less than a radian, so the left-hand side of that inequality approximately sets the maximum step size for exact spin integration. The adiabatic trajectory can handle large rotations per time step but assumes a constant field during the step, so the right-hand side limits the step size for adiabatic spin integration. In this limit, therefore, the adiabatic spin trajectory can be much faster.



A comparison of the outputs from the adiabatic and exact trajectories is shown in figure 2. Note that the exact trajectory becomes increasingly inaccurate as the integration time approaches the precession period $33 \mu\text{s}$, even for 10 ms tracks. There may, however, be other limitations on the step size that prevent this from being the case. In particular, for the UCN tracking described in this work, weak magnetic fields mean that the limiting factor on the time step is error in position, not spin, so adiabatic and exact spin tracking require similar computation time.

In this article, we present our results using both methods. The exact method could be especially applicable in non-adiabatic cases, e.g. tracking the spin-precession of co-magnetometer ^{199}Hg atoms in room temperature neutron EDM experiments [27], where typical magnetic fields of order $\sim 1 \mu\text{T}$ are used. In this case, $\gamma_{\text{Hg}}|\mathbf{B}|\tau_c < 1$, since the ^{199}Hg atoms are relatively hot, where $\tau_c = 2R/v_{\text{RMS}}$, R is the transverse size of the storage chamber, v_{RMS} is the root mean square velocity of the species under consideration (^{199}Hg atoms in this case), and γ is the gyromagnetic ratio of the atoms. On the other hand, in order to track the UCNs in a similar magnetic field environment, one can use the adiabatic method, since $\gamma_n|\mathbf{B}|\tau_c > 1$, owing to the low velocity of the UCNs. This ability to choose the tracking method, allows greater flexibility in the applicability of this toolkit.

4. UCN storage

Having established that the exact and adiabatic spin tracking methods agree under appropriate conditions, we next consider how well Kassiopeia can reproduce experimental data from UCN precession chamber in references [10, 27–29]. The neutron precession chamber under consideration is a cylinder of radius 23.5 cm and height 12 cm . The interior rounded surface is primarily deuterated polystyrene (dPS), with small windows of deuterated polyethylene, while the two flat ends of the cylinder (the electrodes) are covered in diamond-like carbon (DLC).

UCN reflections from surfaces are described by three features: the reflection probability, the depolarization probability, and the distribution of outgoing angles for reflected neutrons. The first two are described in [30], while the third is described in [31]. We will summarize these and discuss our estimates of the associated parameters.

The UCN reflection probability at an energy E and angle to the surface normal θ is given by [32]:

$$P(R) = 1 - \eta \left(\frac{E_{\perp}}{V_f - E_{\perp}} \right)^{1/2}, \quad (8)$$

where $E_{\perp} = E \cos^2 \theta$ is the component of energy from normal momentum, V_f is the real part of the surface's optical potential, and η is another constant of the surface. For dPS, these values are known only approximately, with $\eta \sim (1-3) \times 10^{-4}$ [30] and $V_f \sim 161 \text{ neV}$ [33], while a range of values for DLC is $\eta \sim (0.7-1.7) \times 10^{-4}$ [34] and $V_f \sim 286 \text{ neV}$ [35]. The UCN depolarization probability is the simplest to

describe, and is given by a constant β . For dPS, this is known very roughly as $\beta \sim (1.3\text{--}8.9) \times 10^{-6}$ [30], and again a range of values for DLC is $\beta \sim (0.7\text{--}2.2) \times 10^{-6}$ [34].

Detailed theoretical treatments of the distribution of outgoing angles for reflected UCNs can be found in [31, 32, 36]. Since the behavior of UCNs in the precession chamber should not depend significantly on the exact angular distribution, we derive an approximate form. The angular distribution of stored neutrons is averaged out and does not play an effect in rotationally symmetric storage chambers such as the cylinder considered in this work [16].

The roughness of surfaces leads to non-specular reflection. In our simulation, which involves storage of UCNs in a cylindrical chamber, the role of roughness can be played by adjusting the loss (η) and depolarization (β) parameters [32]. However, non-specular reflection can be much more significant in other contexts, especially in neutron waveguides. We have implemented the micro-roughness model in our toolkit to allow for such simulations.

We start from the micro-roughness model result which, up to a normalization constant, can be modeled as:

$$p(\theta_i, \Phi_f) \propto |S(\theta_f)|^2 \exp \left[-\frac{(wk)^2}{2} (\sin^2 \theta_i + \sin^2 \theta_f - 2 \sin \theta_i \theta_f \cos \Phi_f) \right], \quad (9)$$

Here, θ_i and θ_f are the incident and outgoing angles to the normal, ϕ_f is the change in direction around the normal, w is the surface roughness, k is the neutron wave vector, and,

$$|S(\theta_f)| = \left| \frac{2 \cos \theta_f}{\cos \theta_f + \sqrt{\cos^2 \theta_f - k_c^2/k^2}} \right|, \quad (10a)$$

$$= 2k \cos \theta_f / k_c, \quad (10b)$$

where $k_c = \sqrt{2mV_f/\hbar}$ is the wave number corresponding to the optical potential and we consider only neutrons with $k < k_c$, since higher-energy neutrons quickly escape the precession chamber. Then,

$$p(\theta_i, \Phi_f) \propto \cos^2 \theta_f \exp \left[-\frac{1}{2} (wk)^2 (\sin \theta_i - \sin \theta_f)^2 + (wk)^2 \sin^2 \theta_i (\cos \Phi_f - 1) \right], \quad (11a)$$

$$\approx (1 - \tan \theta_i \Delta\theta) \exp \left[-\frac{(wk)^2}{2} \cos^2 \theta_i \Delta\theta^2 - \frac{(wk)^2}{2} \sin^2 \theta_i \Delta\theta^2 \right], \quad (11b)$$

where we defined $\Delta\theta = \theta_f - \theta_i$. This gives a simple approximate distribution of outgoing angles that can be efficiently sampled. Note that this derivation assumes that the change in incident and outgoing angles is small. This is a rough approximation in our case, but we found that our simulations were insensitive to the exact parameters of the reflected distribution, so this should not significantly affect our results.

For our simulations, we used $\beta = 6 \times 10^{-6}$, $\eta = 1 \times 10^{-4}$, $V_f = 150$ neV, and $w = 30$ nm, which were consistent with the available estimated ranges of each value (see [37, 38] for measurements of w). Note that the first two parameters were chosen so as to be most consistent with data in references [39–42]; we emphasize that we did not attempt simulations with multiple values of these parameters in order to find those most consistent with the measured depolarization timescales and storage times. In the future, it might be possible to use our simulations and the known timescales as a means of actually determining these parameters, but this was beyond the scope of this work. Extraction of these input parameters from the published values of T_1 , T_2 , and storage time constant in references [39–42], respectively, will be a topic of a future article.

For each test simulation, the precession chamber's interior had an essentially constant magnetic field of approximately $1 \mu\text{T}$ along the cylinder radius, with $\mathcal{O}(nT)$ deviations along each coordinate axis. In an experiment dedicated to measuring the electric dipole moment, the apparatus would also contain an electric field in either axial direction, but this was not included in our simulation since electric effects are below the sensitivity of the experiment [28]. The axial magnetic fields were different (and in particular were in opposite directions) for the two electric field directions, and we used a set of magnetic field measurements of each field configuration [44] along with a combination of natural neighbors interpolation (to reach a rectilinear lattice) and cubic interpolation (within lattice cells) to estimate the magnetic field everywhere.

During a particular run of our simulation, a number of neutrons would be added to just above the bottom of the precession chamber. While neutrons may not actually all start near the bottom surface, their motion around the trap is sufficiently fast relative to the simulation times that the choice of the origin location of the neutrons should not affect the results significantly. The initial direction of the neutrons were

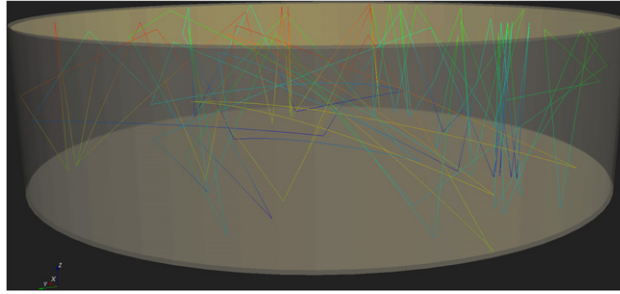


Figure 3. A VTK image of three neutrons tracked for 1 s inside of the precession chamber. Colors correspond to kinetic energies, with higher energies at the blue end of the spectrum. Note the approximately specular reflections and the slight curvature in the tracks induced by gravity.

picked isotropically. For the sake of this simulation, neutron kinetic energies were generated from a Gaussian distribution with a mean of 150 neV and a standard deviation of 50 neV. This is an energy distribution that is harder than the energy distribution estimated in reference [45]. Softening of the energy spectra during storage is chiefly due to the loss of higher energy neutrons. Our simulation includes this loss channel, so the choice of initial energy spectra has a negligible effect on the relative parameters we use to simulate in this paper. It may be possible to match the measured energy distribution more closely by varying the parameters of β , η , V_f and w , described above, but this was beyond the scope of this work. During a given run, all neutrons would also begin with the same spin, which varied by experiment as described below. Three example tracks inside of the simulated precession chamber are shown in figure 3.

5. Results and discussion

We chose to vet the updated Kassiopeia toolkit by simulating UCN storage, since there was experimental data available to benchmark its performance and accuracy. We compared our simulation's results with three previously measured parameters associated with the precession chamber under consideration: the longitudinal relaxation time T_1 [39, 42], the transverse relaxation time T_2 [40, 42], and the effective trap lifetime τ including neutron decay and wall losses [41, 42]. Using a similar simulation but with the converse of the process we have employed here, the parameters of η , V_f and w associated with the trap could be obtained just by using the data of neutron storage loss as a function of storage time alone, as was done in reference [20, 43]. Previous works neglected the effects of depolarization. Particularly, the improvement we present in this work also takes into consideration the effects of depolarization per bounce parameter of β , allowing us to simulate the longitudinal and transverse depolarization rates in addition to the trapping lifetime.

A total of 17 280 neutrons were simulated up to maximum times of 500 s. This was done using four parallel $c4.8\times$ large instances of amazon elastic compute cloud (EC2), or 144 total cores. Kassiopeia does not directly support parallelization of particle tracking, so we instead ran 144 separate simulations of 120 neutrons each and then combined the outputs. This took approximately 2500 CPU-hours, though further optimization is likely possible.

5.1. The longitudinal relaxation time T_1

The longitudinal relaxation time, T_1 , is the time constant of the decay of average polarization for neutrons with initial spins that are either aligned or anti-aligned relative to the local magnetic field. It should be noted that, even for UCNs, the μ T-order magnetic fields in the precession chamber do not significantly affect neutron energies since $\mu_N|\mathbf{B}|$ is far less than the kinetic energy. On a microscopic level, longitudinal relaxation is associated with inhomogeneities of the magnetic field, and with depolarization due to reflections [27].

Since the adiabatic equation of motion (6b) for fully aligned or anti-aligned spins always gives a zero derivative of the aligned spin, our simulations instead started spins at 1° or 179° to the magnetic field, though we found that any angle up to a few degrees led to indistinguishable results, as the dominant contribution to T_1 came from reflection depolarization.

We simulated 4320 neutrons for 500 s using both the adiabatic and exact trajectories with half initially aligned and half initially anti-aligned, and compared our average polarization as a function of time to that obtained in references [39, 42]. Our results can be seen in figure 4, where a relative polarization of 1

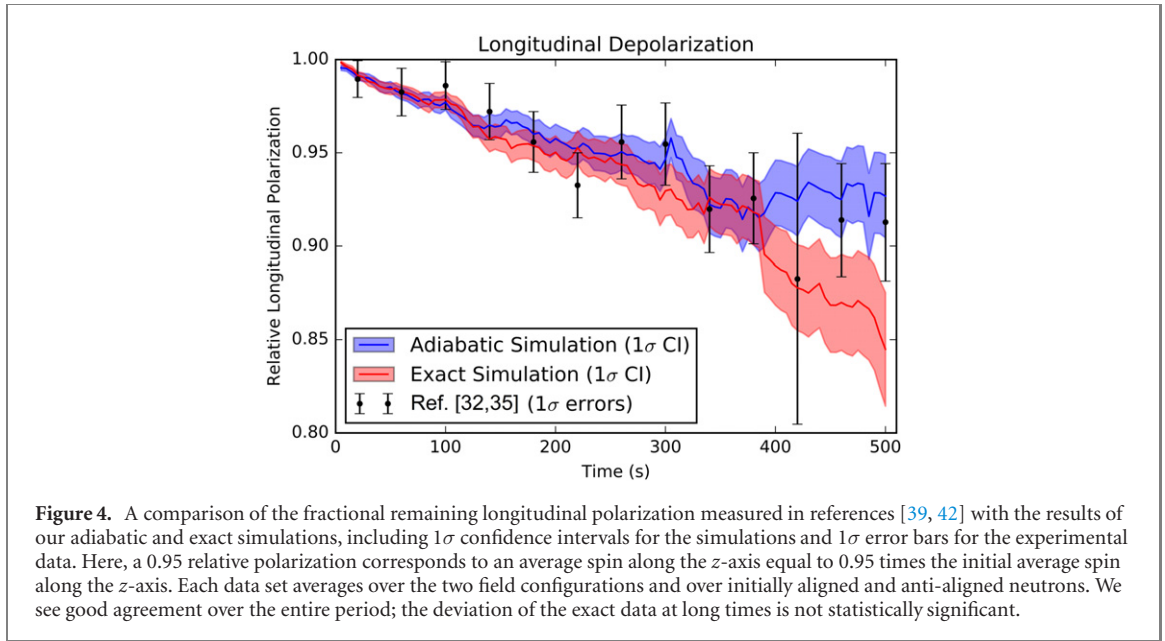


Table 1. The results of χ^2 testing of our results against the experimental data in references [39–42], including left-sided p -values. Since remaining atom counts and polarizations are highly correlated (an upward deviation at one time will tend to lead to upward deviations at later times), ratios of counts and polarizations at successive times were compared instead. The generally small χ^2 values suggest that we are overestimating our errors, though it is unclear how this could be the case. Conversely, the T_1 adiabatic lifetime data’s disagreement with the experimental data may indicate that our assumed value of η was not correct.

Simulation	T_1 or T_2		Lifetime	
	χ^2/ndf	p	χ^2/ndf	p
T_1 Ad	0.22	1.00	2.43	0.02
T_1 Ex	0.66	0.84	0.53	0.90
T_2 Ad	0.13	1.00	0.56	0.88
T_2 Ex	1.29	0.29	0.85	0.66

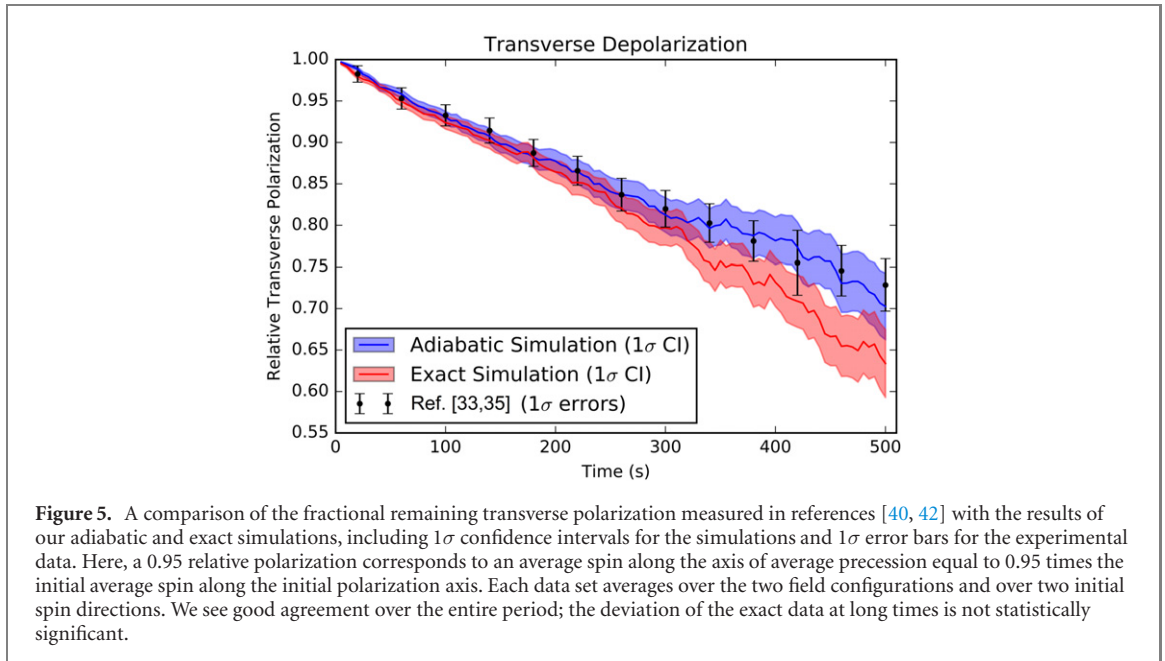
indicates an average polarization equal to the initial value (± 1 in simulations, but smaller magnitudes in references [39, 42]).

As figure 4 shows, both the adiabatic and exact simulations were able to accurately reproduce the measured longitudinal depolarization rate. Both simulations are within 1σ of the experimental data (using the combined error) until around 350 s, and the adiabatic simulations continue to closely match the experiment for the entire run. The apparent discrepancy between the experimental data and the exact trajectory at high times is not statistically significant (see table 1).

5.2. The transverse relaxation time T_2

The transverse relaxation time, T_2 , is the time constant of the decay of average polarization for neutrons with initial spins that are aligned along an axis perpendicular to the local magnetic field. The dominant contribution to transverse relaxation of neutrons in the precession chamber is the variation in the magnetic field over the trap volume [27]. Note that spin–spin interactions, which may be the dominant contribution to T_2 in other contexts, are not significant for neutrons in this context owing to their low density [46]. However, spin–spin interactions between two neutrons cannot be implemented in Kassiopeia at this time, as it tracks particles one at a time.

In the T_2 measurements reported in references [40, 42], neutrons began with polarizations aligned or anti-aligned with the magnetic field and then T_2 was measured between two $\pi/2$ pulses that rotated them into and out of the perpendicular plane defined by the direction of the main $\sim 1 \mu\text{T}$ holding magnetic field. While ideal spin rotating pulses are implemented in Kassiopeia, they were not used for this simulation since we were interested only in the behavior occurring within the field-perpendicular plane.



We simulated 4320 neutrons for 500 s using both trajectory types and two different initial spin directions perpendicular to the magnetic field. We then compared our average polarization as a function of time to that obtained in references [40, 42]. Our results can be seen in figure 5, with relative polarization defined as for T_1 , but along the axis corresponding to average precession over that time instead of along the z -axis.

As figure 5 shows, both simulations were also able to accurately reproduce the measured transverse depolarization rate. The adiabatic simulation matches all of the experimental values, however the exact simulation results appear to deviate from the data at long times. However, this discrepancy is again not statistically significant (see table 1), as our simulation errors are highly correlated: neutrons that deviate significantly from the average polarization (due to depolarization on reflection, for example) are likely to remain in the trap for some time, lowering the average polarization at those later times as well.

5.3. The effective trap lifetime τ

Since neutron reflection from material surfaces is not guaranteed, especially at higher energies (see equation (8)), the effective lifetime of neutrons in the precession chamber is significantly lower than their decay lifetime. Neutrons may also be lost due to holes or other imperfections in a physical trap. Storage lifetimes may be extracted independently from both the simulations dedicated to T_1 or T_2 , but the storage lifetime should be nearly independent of the neutrons' spins in a $\sim 1 \mu\text{T}$ field. The results from both sets of simulations, as well as from references [41, 42], are shown in figure 6.

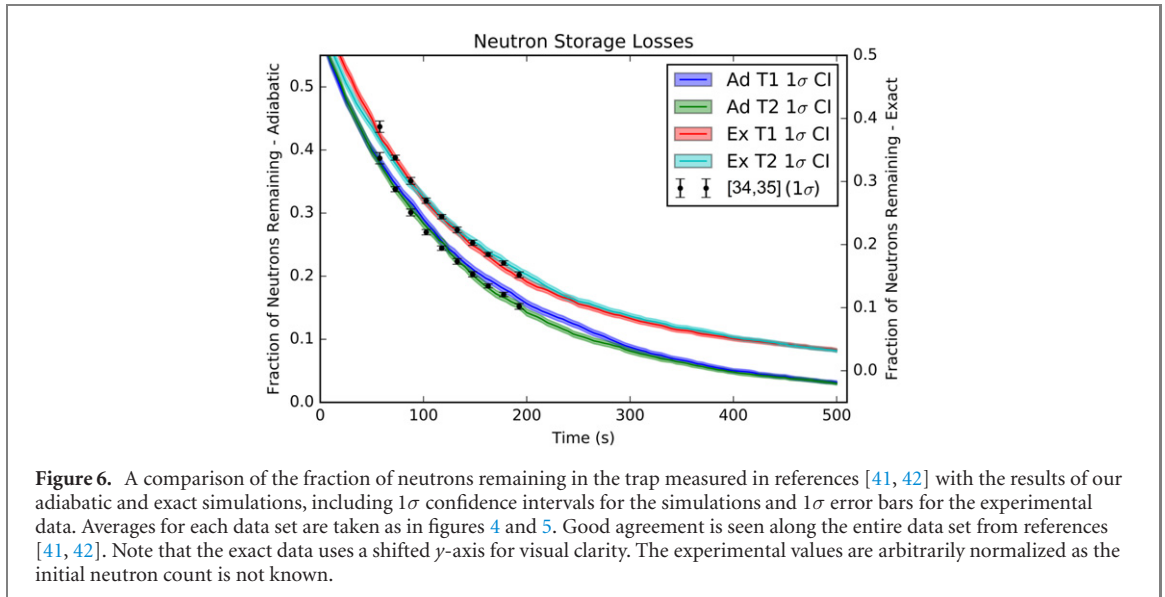
Figure 6 once again shows good agreement between each of the four simulations and the experimental data. The adiabatic T simulation deviates significantly from the experimental data (see table 1), but the lifetime is strongly dependent on the chosen value of η and the initial energy distribution—both of which are known with limited precision for the chamber under consideration—so this discrepancy is not practically significant.

5.4. Summary of results

A summary of our simulated data's agreement to the experimental data in references [39–42] is presented in table 1, showing generally good agreement. The apparent overestimation of errors is expected to be the result of correlations between our errors at different times. This demonstrates that Kassiopeia can reproduce the effective lifetime as well as both decoherence times for neutrons within a precession chamber, confirming that it can accurately simulate neutral particles.

5.5. Comparison of the simulation toolkits

As other authors have noted before us [16], it is critical to have multiple simulation toolkits to allow for comparisons and thereby build confidence in the physics results. Kassiopeia toolkit offers a versatile new resource to augment the various existing simulation toolkits. In this sub-section, we compare the features and validation strategies of other toolkits while highlighting the advantages of the updated Kassiopeia toolkit.



All of the other toolkits, i.e. Geant4 [11, 12], PENTrack [13], STARucn [14, 15] and MCUCN [16], are limited to slowly varying fields to accommodate the adiabatic case. Additionally, all but the PENTrack toolkit are restricted to weak fields, and are unable to simultaneously simulate co-magnetometer atoms. Kassiopeia allows for non-adiabatic systems to be simulated. While PENTrack does allow certain co-magnetometer atoms to be simulated, our new Kassiopeia package is built to handle neutral particles, atoms, and molecules. Given that most co-magnetometer species are in fact non-adiabatic systems, Kassiopeia is the only toolkit currently available that is able to realistically simulate co-magnetometer atoms. Furthermore, while MCUCN and PENTrack have implemented reflection over rough surfaces, it is left up to the user to extraneously add roughness to materials in Geant4UCN and StarUCN, in order to simulate non-specular reflection. Also, MCUCN and StarUCN require magnetic fields defined as a combination of basic volumetric shapes. In Kassiopeia (and PENTrack), generic finite element field maps can be directly used.

Previous neutron simulation toolkits have taken a variety of approaches to verifying their simulation results. In order to validate Geant4UCN, reference [11] compares their simulation results—collision frequencies and transmission in a neutron guide—with prior numerical code. Similarly, StarUCN [14] has compared various scenarios with MCUCN and Geant4UCN. PENTrack [13] has presented comparisons of transmission in neutron guide and neutron absorption in foils and absorbers with Geant4UCN and StarUCN. MCUCN [16], on the other hand, presents comparisons with analytic solutions for the evolution of the energy spectra and center-of-mass of the ensemble of stored UCNs.

No previous toolkits has presented checks involving spin precession tracking, as we have done here by vetting the depolarization time constants using the Kassiopeia toolkit. In this article, we have presented comparisons between Kassiopeia results and real world data, demonstrating the capabilities of this new toolkit.

6. Other applications

Having established that Kassiopeia can accurately simulate neutral particles' motion in at least one context, we next consider a few potential future applications of these features.

The application most directly stemming from the simulations in this paper is simulated prototyping of future UCN experiments [47–51]. In this work, we simulated neutron precession using a previously measured magnetic field, but Kassiopeia also includes extensive field calculation methods, which can be used to calculate the magnetic fields inside of a trap based on its design [18, 19]. Kassiopeia could therefore be used to estimate the effective lifetime and relaxation times of future UCN experiments.

Such simulation toolkits are vital in the analysis of many experimental results, and provide inputs that are an integral part of the final result. For example, searches for neutron to mirror-neutron oscillations depend on the mean time-of-flight of the stored neutrons inside the chamber. The mean time-of-flight, in turn, depends intimately on the time evolution of the energy spectra of the stored neutrons. A simple model involving a single loss-coefficient for the entire chamber was simulated using MCUCN to extract the energy evolution and thereby the mean time-of-flight of the stored neutrons in references [20, 43]. Kassiopeia can

further improve such simulations by performing realistic simulations of co-magnetometer atoms simultaneously with UCNs.

Neutron simulations have, in fact, already had an impact on measurements of the neutron lifetime. Several Monte Carlo (MC) simulations have been developed to model the early UCN experiments that used material storage bottles [21, 22]. These MC simulations have adjusted the corresponding lifetime by a few seconds, reducing the tension between the beam and the bottle lifetime measurements [23, 24]. There are no independent simulations verifying the claims of these MCs, however. The Kassiopeia toolkit may be able to provide a new, comprehensive check of these results.

Another potential application is simulating tritium storage methods in the Project 8 neutrino mass experiment [52]. Currently, atomic tritium is stored using a purely magnetic trap. We have previously simulated versions of this trap in order to obtain estimates of necessary currents and effective lifetimes, but development of the final trap configuration is ongoing and further simulation work could be done in this area. Furthermore, one current proposal is to use a combined magneto-gravitational trap instead, which has not been simulated as of writing.

Neutral particle simulation can also be applied to atomic experiments. Experiments such as ACME [53] and others such as [54] use molecular beams to measure the electric dipole moment. Molecules are prepared in particular spin states and then precess through constant electric and magnetic fields; a dependence of precession on the electric field can indicate an electric dipole moment. Kassiopeia may be able to simulate molecular evolution within these fields to aid with estimating systematic errors.

Acknowledgments

The authors would like to thank Mathieu Guigue for some helpful discussion. We would also like to acknowledge the support from the KATRIN and the Project 8 collaborations. This work was supported by the MIT Undergraduate Research Opportunities Program, by the Department of Energy Office of Nuclear Physics under Award No. DE-SC0011091, and by SERI-FCS under Award No. 2015.0594. Other allied works were supported by Sigma Xi under Grant Nos. G2017100190747806 and G2019100190747806.

Data availability statement

The data that support the findings of this study are available upon reasonable request from the authors.

ORCID iDs

P Mohanmurthy  <https://orcid.org/0000-0002-7573-7010>

J A Formaggio  <https://orcid.org/0000-0002-3757-9883>

References

- [1] Zel'dovich Y B 1959 Storage of cold neutrons *Sov. Phys.-JETP Lett.* **9** 1952–3
- [2] Lushchikov V I *et al* 1969 Observation of ultracold neutrons *JETP Lett.* **9** 23–40
- [3] Steyerl A 1969 Measurements of total cross sections for very slow neutrons with velocities from 100 m s^{-1} to 5 m s^{-1} *Phys. Lett. B* **29** 33
- [4] Pattie R W *et al* 2018 Measurement of the neutron lifetime using a magneto-gravitational trap and in situ detection *Science* **360** 627
- [5] Serebrov A P *et al* 2008 Neutron lifetime measurements using gravitationally trapped ultracold neutrons *Phys. Rev. C* **78** 035505
- [6] Mumm P 2018 Resolving the neutron lifetime puzzle *Science* **360** 605
- [7] Mannel T 2007 Theory and phenomenology of CP violation *Nucl. Phys. B* **167** 170
- [8] Abel C *et al* 2017 Search for axionlike dark matter through nuclear spin precession in electric and magnetic fields *Phys. Rev. X* **7** 041034
- [9] Altarev I *et al* 2011 New constraints on Lorentz invariance violation from the neutron electric dipole moment *Europhys. Lett.* **92** 51001
- [10] Abel C *et al* 2020 Measurement of the permanent electric dipole moment of the neutron *Phys. Rev. Lett.* **124** 081803
- [11] Atchison F *et al* 2005 The simulation of ultracold neutron experiments using GEANT4 *Nucl. Instrum. Methods Phys. Res. A* **552** 513
- [12] Allison J *et al* 2016 Recent developments in Geant4 *Nucl. Instrum. Methods Phys. Res. A* **835** 186
- [13] Schreyer W *et al* 2017 PENTrack—a simulation tool for ultracold neutrons, protons, and electrons in complex electromagnetic fields and geometries *Nucl. Instrum. Methods Phys. Res. A* **858** 123
- [14] Clément B and Roulier D 2014 StarUCN (<https://sourceforge.net/projects/starucn>)
- [15] Ayres N J *et al* 2018 Monte Carlo simulations for the optimization and data analysis of experiments with ultracold neutrons *JPS Conf. Proc. (NOP 2017)* vol 22

- [16] Zsigmond G 2018 The MCUCN simulation code for ultracold neutron physics *Nucl. Instrum. Methods Phys. Res. A* **881** 16
- [17] Furse D et al 2017 Kassiopeia: a modern, extensible C++ particle tracking package *New J. Phys.* **19** 053012
- [18] Corona T J 2009 Tools for electromagnetic field simulation in the KATRIN experiment *Master's Thesis* Massachusetts Institute of Technology
- [19] Barrett J P 2017 A spatially resolved study of the KATRIN main spectrometer using a novel fast multipole method *PhD Thesis* Massachusetts Institute of Technology
- [20] Mohanmurthy P 2020 A search for neutron to mirror-neutron oscillations *PhD Thesis* ETH Zürich
- [21] Serebrov A P and Fomin A K 2009 Monte Carlo simulation of quasi-elastic scattering and above-barrier neutrons in the neutron lifetime experiment MAMBO I *JETP Lett.* **90** 555
- [22] Serebrov A P and Fomin A K 2010 Neutron lifetime from a new evaluation of ultracold neutron storage experiments *Phys. Rev. C* **82** 035501
- [23] Serebrov A P 2019 Neutron lifetime: experimental problem or anomaly? *J. Phys. Conf. Ser.* **1390** 012007
- [24] Serebrov A P et al 2021 Search for explanation of the neutron lifetime anomaly *Phys. Rev. D* **103** 074010
- [25] Jackson J D 1999 *Classical Electrodynamics* 3rd edn (New York: Wiley)
- [26] Littlejohn R G and Weigert S 1993 Adiabatic motion of a neutral spinning particle in an inhomogeneous magnetic field *Phys. Rev. A* **48** 924
- [27] Abel C et al 2019 Magnetic field uniformity in neutron electric dipole moment experiments *Phys. Rev. A* **99** 042112
- [28] Baker C A et al 2014 Apparatus for measurement of the electric dipole moment of the neutron using a cohabiting atomic-mercury magnetometer *Nucl. Instrum. Methods Phys. Res. A* **736** 184
- [29] Abel C et al 2019 nEDM experiment at PSI: data-taking strategy and sensitivity of the dataset *EPJ Web Conf. (PPNS 2018)* vol 219
- [30] Chesnevska S 2007 Investigation of electric fields, losses and depolarization of ultra-cold neutrons for the new nEDM experiment at FRM II *PhD Thesis* Technischen Universität München
- [31] Atchison F et al 2010 Diffuse reflection of ultracold neutrons from low-roughness surfaces *Eur. Phys. J. A* **44** 23
- [32] Golub R, Richardson D and Lamoreaux S K 1991 *Ultra-Cold Neutrons* (Boca Raton, FL: CRC Press)
- [33] Bondar V et al 2017 Losses and depolarization of ultracold neutrons on neutron guide and storage materials *Phys. Rev. C* **96** 035205
- [34] Atchison F et al 2007 Loss and spinflip probabilities for ultracold neutrons interacting with diamondlike carbon and beryllium surfaces *Phys. Rev. C* **76** 044001
- [35] Atchison F et al 2007 Measurement of the Fermi potential of diamond-like carbon and other materials *Nucl. Instrum. Methods Phys. Res. B* **260** 647
- [36] Steyerl A 1972 Effect of surface roughness on the total reflexion and transmission of slow neutrons *Z. Phys. A* **254** 169
- [37] Ting Y-H et al 2010 Surface roughening of polystyrene and poly(methyl methacrylate) in Ar/O₂ plasma etching *Polymers* **2** 649
- [38] Dongping L, Yanhong L and Baoxiang C 2006 Surface roughness of various diamond-like carbon films *Plasma Sci. Technol.* **8** 701
- [39] Helaine V 2014 Neutron electric dipole moment measurement: simultaneous spin analysis and preliminary data analysis *PhD Thesis* Université de Caen
- [40] Zenner J 2013 The Search for the neutron electric dipole moment *PhD Thesis* Johannes Gutenberg-Universität
- [41] Abel C et al 2019 Statistical sensitivity of the nEDM apparatus at PSI to neutron mirror-neutron oscillations *EPJ Web Conf. (PPNS 2018)* vol 219
- [42] Mohanmurthy P 2021 Characterization of PSI nEDM apparatus: T_1 , T_2 , and UCN storage lifetime *Internal Technical Report, DSpace at MIT* (MIT Libraries)
- [43] Abel C et al 2021 A search for neutron to mirror-neutron oscillations using the nEDM apparatus at PSI *Phys. Lett. B* **812** 135993
- [44] Wyszynski G 2015 Development of magnetic field control system in the nEDM experiment *PhD Thesis* Jagiellonian University
- [45] Afach S et al 2015 Observation of gravitationally induced vertical striation of polarized ultracold neutrons by spin-echo spectroscopy *Phys. Rev. Lett.* **115** 162502
- [46] Bison G et al 2017 Comparison of ultracold neutron sources for fundamental physics measurements *Phys. Rev. C* **95** 045503
- [47] Abel C et al 2019 The n2EDM experiment at the Paul scherrer institute *EPJ Web Conf. (PPNS 2018)* vol 219
- [48] Ahmed S et al ((TUCAN Collaboration) 2019 First ultracold neutrons produced at TRIUMF *Phys. Rev. C* **99** 025503
- [49] Ito T M et al 2018 Performance of the upgraded ultracold neutron source at Los Alamos national laboratory and its implication for a possible neutron electric dipole moment experiment *Phys. Rev. C* **97** 012501
- [50] Wurm D et al 2019 The PanEDM neutron electric dipole moment experiment at the ILL *EPJ Web of Conf. (PPNS 2018)* vol 219
- [51] Serebrov A 2017 Present status and future prospects of N-EDM experiment of PNPI-ILL-PTI collaboration *Proc. Science (INPC2016)* vol 281
- [52] Esfahani A A et al (Project 8 Collaboration) 2017 Determining the neutrino mass with cyclotron radiation emission spectroscopy—Project 8 *J. Phys. G* **44** 054004
- [53] Baron J et al (ACME Collaboration) 2014 Order of magnitude smaller limit on the electric dipole moment of the electron *Science* **343** 269
- [54] Hudson J J et al 2011 Improved measurement of the shape of the electron *Nature* **473** 493